Research Article

Shumei Lou*, Hui Zhang, Fang Liu, Jianchao Wang, Wenying Yin, Zhiyuan Chen and Chunjian Su

Performance improvements of a short glass fiber-reinforced PA66 composite

https://doi.org/10.1515/secm-2021-0045
received March 24, 2021; accepted August 03, 2021

Abstract: A plate used in a medium voltage switch, made by a 25 wt% glass fiber-reinforced polyamide 66 composite filled with flame-retardant red phosphorus (RP) (PA66-GF25 FR (RP)), was injection molded. To satisfy the relatively high dimensional accuracy requirement, a "supporting mold" was used to compensate for the difference between the transverse and longitudinal linear shrinkage of the PA66-GF25 FR (RP). To reduce the internal residual stress caused by the "supporting mold," hygrothermal conditioning treatments, including boiling water bath at 90–100°C and re-drying at 110°C, were used. To determine the effects of boiling water bath and re-drying on the dimensional accuracy and mechanical properties of the product, three treatment routes were applied. It was found that the route in which the boiling water bath is applied after the "supporting mold" is preferred to ensure the dimensional accuracies and the mechanical properties as a whole. Using a boiling water bath as a hygrothermal conditioning treatment can improve the mechanical properties and increase the dimensional accuracy of the product. In addition, by using the preferred route, re-drying can further improve the tensile, bending, and even impact strength.

Keywords: PA66-GF25 FR (EP), injection molding, boiling water bath, mechanical property, dimensional accuracy

1 Introduction

Polyamide 66 (PA66) has excellent comprehensive mechanical properties and is widely used in automobiles, electronics, machinery, chemistry, and other fields. However, to improve the chemical, corrosion, mechanical, and heat resistance [1–4], reinforcing phase, such as glass fibers (GFs), is added to the PA66 matrix to manufacture glass fiber-reinforced composites (e.g., glass fiber-reinforced PA66 composites, PA66-GF).

PA66-GF is used to produce electrical insulation components, which require good flame-retardant properties. However, GFs are likely to cause sustained combustion phenomena, such as "candle wicking." Thus, some flame retardants are added to PA66-GF to improve the flame-retardant properties. Red phosphorus (RP) is considered to be one of the best fire retardants for obtaining perfect dielectric and flame-retardant properties, which are seriously important properties for electrical insulation components [5–7].

Besides flame-retardant properties, dimensional accuracies and mechanical properties are also important for both assembly and structural performance of electrical insulation components. It has been observed that RP has few effects on the mechanical properties and dimensional stability of polyamide composites [6,7]. The dimensional accuracies and the mechanical properties of fiber-reinforced polyamide products are influenced by the injection molding process conditions [8–10] and the environmental conditions such as moisture and temperature [10–16]. The dimensional accuracies and mechanical properties of fiber-reinforced polyamide products are influenced by moisture and temperature because PA66 has a high polarity and tends to absorb water molecules to form hydrogen bonds. Especially in a high-temperature and high-humidity environment, the moisture absorption rate of PA66 is high, and this affects the dimensional stability of the product. Many researchers have found that polyamide swells in the hygrothermal aging process [12,13,17,18], and the mechanical properties degrade in general at the same time. Water conditioning is always

* **Corresponding author: Shumei Lou,** Department of Mechanical and Electrical Engineering, Shandong University of Science and Technology, 266590, Qingdao, China, e-mail: msl7119@163.com
Hui Zhang, Wenying Yin, Zhiyuan Chen, Chunjian Su: Department of Mechanical and Electrical Engineering, Shandong University of Science and Technology, 266590, Qingdao, China
Fang Liu, Jianchao Wang: Shandong Taikai Electrical Insulation Co., Ltd, Shandong Taikai High Vol Switchgear Group Co., Ltd., Taian, 271000, China

used to promote saturation, ensuring dimensional stability in subsequent application [12,13]; however, water absorption may degrade the interfacial bonds between the GFs and the polyamide, consequently decreasing the tensile or bending strength of the composite [19–23]. Annealing at 25–35°C below the heat deflection temperature or at 20–35°C above the application temperature can improve some of the mechanical properties of the glass fiber-reinforced polyamide [15,24]. As mentioned earlier, it can be indicated that different hygrothermal conditioning treatments can lead to different dimensional stabilities and mechanical properties [25], which mainly depend on the combined effects of water molecules [19,22], crystallinity [15,19,25], crystal structure phase transition of polyamide [13,25–28], and, perhaps the most important, the interfacial bonding [19–22] between GFs and polyamide. In some studies [19,25], some mechanical properties of the PA66 or PA6 composites were also found to be improved by hygrothermal aging for a relatively short period of time. Moreover, redrying after hygrothermal conditioning was found to further improve the mechanical properties [18].

In this research, an injection molded plate used in a medium voltage switch and made by 25 wt% glass fiber-reinforced PA66 filled with flame retardant RP (PA66-GF25 FR (RP)) based on the dimensional accuracy, surface precision, and flame-retardant performance requirements is studied. To improve the dimensional accuracy, surface quality, and the mechanical properties of the plate, especially of the intermediate circular hole, a "supporting mold" and a hygrothermal conditioning treatment by boiling water bath followed with re-drying are used. Three different treatment routes are used depending on the order of the supporting mold and the boiling water bath. By combining the dimensional measurement, mechanical property test, and micro-morphology analysis, the transverse and longitudinal dimensional accuracies and the mechanical properties of the plate treated by the three treatment routes were compared and analyzed. The best routes were confirmed, in which the dimensional accuracy was improved to satisfy the requirements, ensuring the mechanical properties of the product for the application demand at the same time.

2 Injection molding

2.1 Materials and dimension of the plate

The PA66-GF25 FR (RP) composite (Ultramid® A3X2G5) used in this article is bought from BASF (Germany), and its properties are presented in Table 1.

The dimension and tolerance requirements of the plate are shown in Figure 1, and the thickness of the plate is 6 mm. For convenience, the longitudinal dimension of the product is collectively referred to as "LD," the transverse dimension is collectively referred to as "TD," and the diameter of the central hole is referred to as "DD."

2.2 Mold structure and its gate location

The injection mold of the plate is shown in Figure 2. As shown in Figure 1, the dimensional accuracy of DD is high due to the assembly precision requirements, so the

Table 1: Properties of the PA66-GF25 FR (RP) composite

Typical values at 23°C	Units	Values
Physical properties		
Density	kg/m^3	1,340
Moisture absorption, equilibrium 23°C/50% RH	%	1.20–1.60
Melting temperature, DSC	°C	260
Melt volume rate, MVR 275/5	cm^3/10 min	30
Mechanical properties dry/wet		
Tensile modulus	MPa	8,000/6,000
Tensile strength	MPa	140/100
Fracture strain	%	3/4.5
Impact strength	kJ/m^2	65/70

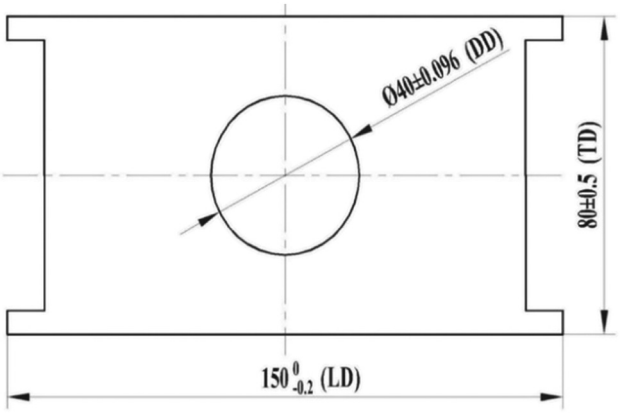

Figure 1: Dimension and tolerance requirements of the plate (unit: mm).

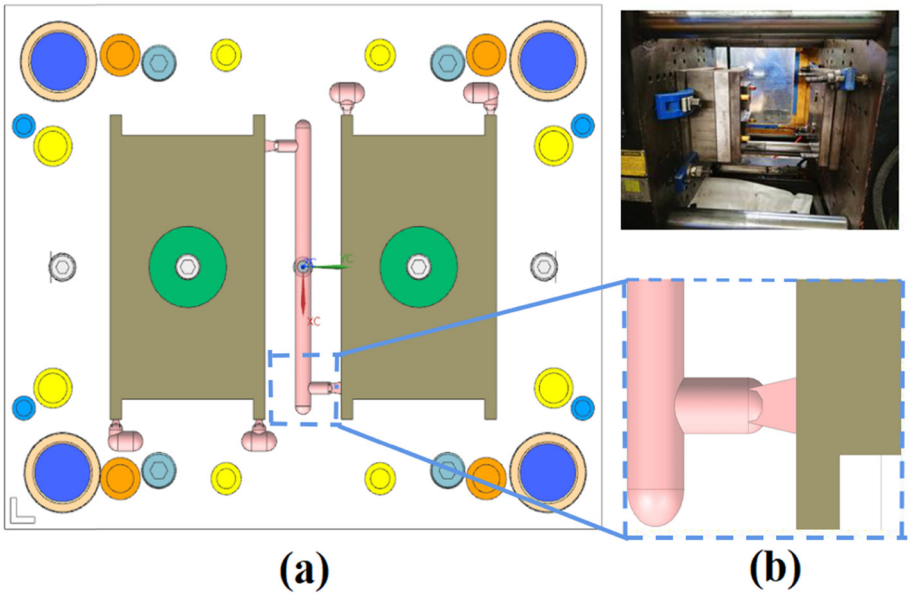

Figure 2: Injection mold: (a) Layout and (b) Gate.

gate must be located at the region far away from the central hole (as shown in Figure 2); environments with medium voltages (approximately 10 kV) require a plate to prevent tip discharge and puncture. Therefore, in the injection molding process, internal void or burrs on the surface cannot exist. Therefore, top plate ejection was used to eliminate the thimble trace in the mold design.

2.3 Process parameters

Before injection molding, the composite is dried at 100°C for 4 h. The temperature of the injection molding machine from the hopper to the nozzle is divided into three segments; more precisely, the ranges of temperatures of the first, second, and third segment are 275–285, 260–275, and 250–265°C, respectively, while the injection pressure is 85 MPa, the dwell time is 3 s, and the injection speed is 50 mm/s.

3 Experimental

3.1 Treatments after injection molding

The volume shrinkage ratio in the initial mold design is 0.5%. After the injected plates are naturally cooled, the initial properties of the plate are obtained through experimental tests. The dimensional accuracies and mechanical properties of the plate meet the engineering requirements, as shown in Figure 1 and Table 2, respectively. However, afterward, the plate continued to shrink, mainly in the following 24 h, and the central circular hole becomes approximately elliptical, as shown in Figure 3(a). This phenomenon is caused by the different longitudinal and transverse linear shrinkage due to the anisotropy of the composite [11] determined by the flowing direction during the injection molding process.

To improve the dimensional accuracy of the central circular hole, a linear shrinkage compensation is necessary. Two methods are typically used to compensate for

Table 2: Initial properties of the plate before adding the "supporting mold"

Samples	Tensile strength (MPa)	Bending strength (MPa)	Impact strength (kJ/m^2)	Elongation (%)	Flame retardation (grade)
1	81	72.5	64	4.4	V-0
2	80	74	67	4.4	V-0
3	82	73	64	4.5	V-0
4	80	75	66	4.3	V-0
5	83	77.5	67	4.5	V-0

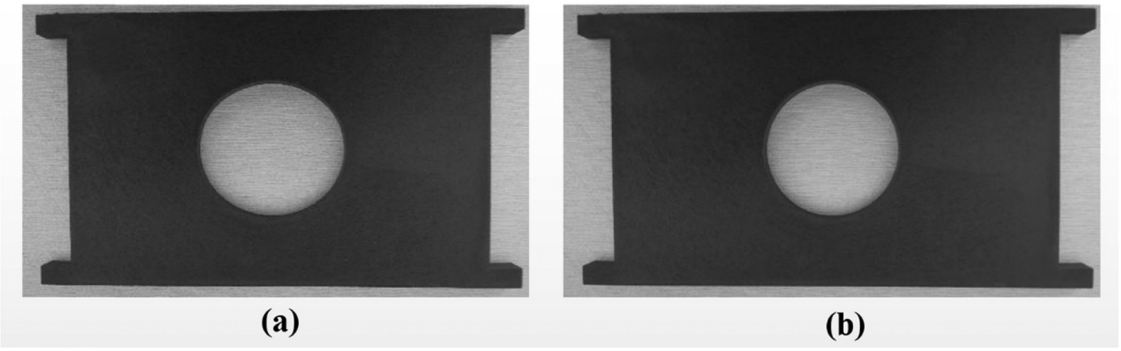

Figure 3: The shape of the central circular hole of the plate: (a) without the "supporting mold" and (b) with the "supporting mold."

the linear shrinkage. One method is to modify the mold size according to the transverse and longitudinal shrinkage ratios; the other method is to apply an external force to limit linear shrinkage after demolding. Since it is difficult to separately consider the longitudinal and transverse shrinkage for the circular holes, the second method is chosen. A cylindrical "supporting mold" with a diameter of 40.024 mm (the initial volume shrinkage is considered) is added into the central circular hole of the plate after demolding and cooling. After compensating for the shrinkage, the longitudinal and transverse dimensions of the central circular hole basically meet the dimensional accuracy requirements, as shown in Figure 3(b). However, at the same time, the mechanical property of the plate is found to decrease by 50%, as presented in Table 3, which is mainly due to the internal residual stress caused as the linear shrinkage is hindered by the "supporting mold."

To eliminate the internal residual stress and to improve the mechanical properties and dimensional accuracy of the plate, boiling water bath (90–100°C, 2 h) is carried out on the plate. Boiling water bath combines the influences of annealing [15,24] and water conditioning saturation [19,25]. To verify the effect of boiling water bath, three treatment routes are applied and compared. Route I involved boiling water bath alone, route II involved boiling water bath after adding a "supporting mold," and route III involved adding a "supporting mold" after boiling water bath, as shown in Figure 4.

Dimensional measurement, mechanical property testing, and micro-morphology analysis of the tensile fracture surface are carried out for the plate treated by the three treatment routes. Ten samples were taken for each route; half of the samples were undried, and the others were dried to study the effects of re-drying [19] on the dimensional accuracy and mechanical properties of the composite. Re-drying is performed in a vacuum oven at a temperature of 110°C for 6 h. The dimensional measurements and mechanical property tests were carried out for the samples before and after re-drying.

3.2 Characterization

The specimen dimensions for the tensile, bending, and impact tests are determined according to GB/T 16491-2008, GB/T 9341-2008, and GB/T 9341-2008, respectively, as shown in Figure 5. These samples were cut along the longitudinal direction of the plate on both sides of the central hole, keeping away from the "weld line." The values of the tensile and bending strengths, elastic modulus, and elongation at break are measured on a CMT5105 universal testing machine (Mattes Industrial Systems Co., Ltd., China). The test speed is 5 mm/min. The impact strength was determined on an XJU-5.5 cantilever beam impact testing machine (Jinan Hengxu Testing Machine Technology Co., Ltd). The impact speed was 3.5 m/s, and the pendulum energy was 5.5 J.

The structural characterization of the plates (untreated and treated by the three routes) were carried out by X-ray diffraction (XRD, D/max-2500/PC, Japan). Data were

Table 3: Mechanical properties of the plates treated with the "supporting mold"

Samples	Tensile strength (MPa)	Bending strength (MPa)	Impact strength (kJ/m^2)	Elongation (%)	Flame retardation (grade)
1	49	67.35	64	5	V-0
2	45	64	60.5	5	V-0
3	50	65	60	4.7	V-0
4	48	65.6	61	4.8	V-0
5	47	66	62.5	5	V-0

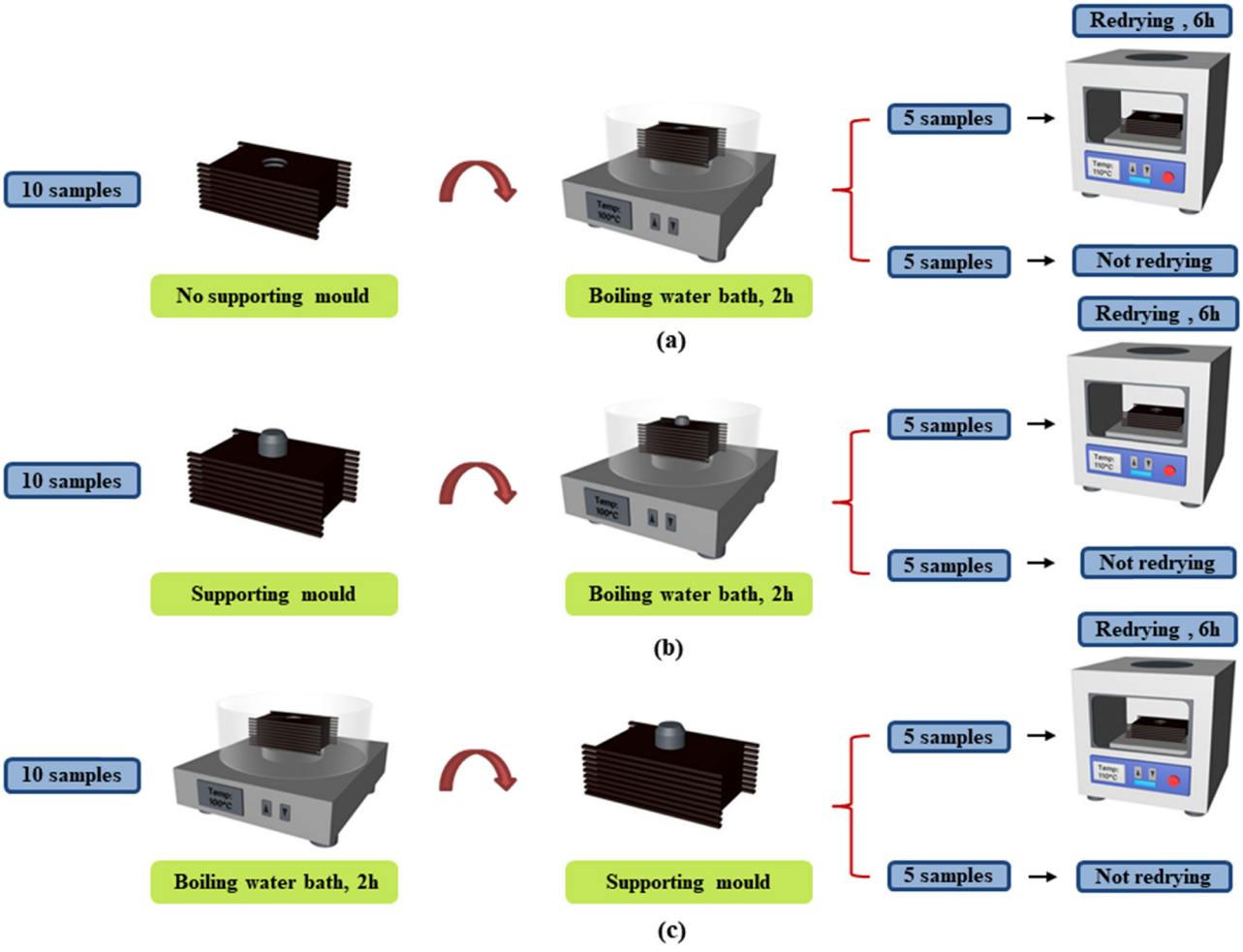

Figure 4: The three routes after injection molding: (a) I, (b) II, and (c) III.

collected over the range $2\theta = 10–40°$ in the fixed time mode with a step interval of 0.02.

The tensile fractured surfaces of the samples treated by the three routes were coated with gold to prevent electrical charging. The surface morphological images of all samples were observed by using scanning electron microscopy (SEM; Sigma 300, Germany) at an acceleration voltage of 5.0 kV.

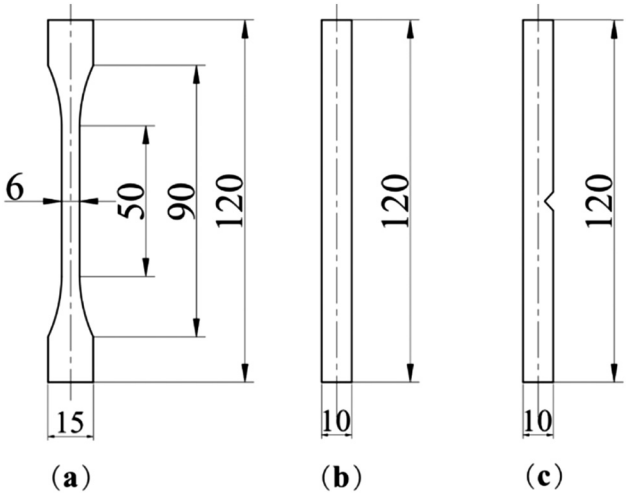

Figure 5: Standard samples size for (a) tensile, (b) bending, and (c) impact testing.

4 Results and discussion

4.1 Dimensional accuracies of the plate treated by the three routes

The dimensions of the plate were measured as described in Section 3 and combined with the shrinkage formula for the injection products (Equation 1) to study accuracies in

the periphery dimensions and the central hole diameter of the plate treated by the three routes.

$$S_L = \frac{L_m - L_p}{L_m} \times 100\%, \quad (1)$$

where S_L is the shrinkage ratio of the injection molded products, L_m is the mold cavity size (the real size after considering the shrinkage volume compensation of 0.5%), and L_p is the size of the injection molded products.

Performing measurements using a micrometer showed that the dimensional accuracies were improved after the three treatment routes; however, there exist some nonnegligible differences between the accuracies obtained with the three routes.

4.1.1 Dimensional accuracy of the central hole

Figure 6 shows the diameter of the central hole (named "DD"), which was measured in the transverse and longitudinal directions of the plate (referred to as "DD_T" and "DD_L," respectively) after the treatments by the three routes. Figure 6(a) and (b) show the DD_T of the undried and the dried parts, respectively, while Figure 6(c) and (d) show the DD_L of the undried and dried parts, respectively. It can also be seen that differences between the "DD_T" and "DD_L" for samples treated by route I without a "supporting mold" are the largest, and the values of "DD_T" and "DD_L" for the undried or dried parts are all out of the tolerance ranges. This result shows that the

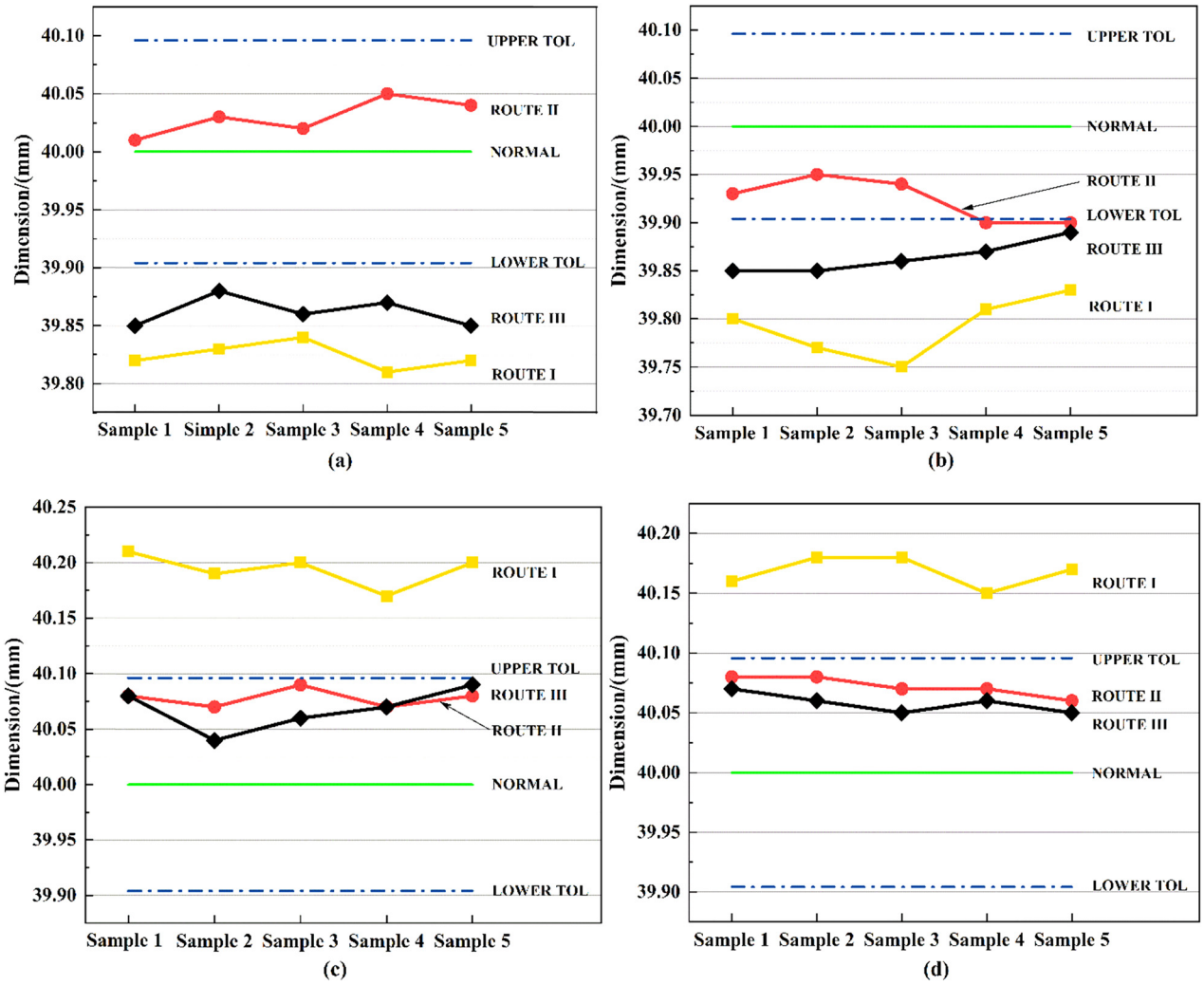

Figure 6: The central hole diameter of the plate by the three routes: (a) DDT, undried parts, (b) DDT, dried parts, (c) DDL, undried parts, and (d) DDL, dried parts.

"supporting mold" can reduce the difference in the shrinkage of the central hole in the two directions, thus increasing the dimensional accuracy. Boiling water bath can relieve the linear shrinkage, which occurs because of hygroscopic expansion that occurs when water is inserted into polyamide composites [11,12,16,17]. Thus, after the treatment, the size of the undried parts expands to be much closer to the nominal size. However, after re-drying, the parts shrink again, which indicates that re-drying prevents the plate from swelling during boiling in the water bath [18]. The dimensional accuracies obtained by route II are higher than route III for both the undried and dried parts.

4.1.2 Periphery dimensional accuracies

Figure 7 shows the average periphery dimension of the plate after the treatment by each route. Figure 7 shows that the peripheral dimensional accuracy of the undried parts is also obviously higher than that of the re-dried ones. Second, the transverse shrinks are much more than the longitudinal ones. Furthermore, the transverse dimension of the plate decreases gradually from the gate side to the nongate side, which means that the shrinkage of the nongate end is the most obvious. As the composite is injected, the pressure far away from the gate is lower than that close to the gate; thus, filling on this side is insufficient, resulting in more severe shrinkage far from the gate than close to the gate. Finally, through the comparison of Figure 7(a)–(c), it can be seen that the transverse dimensions of the undried parts treated by route II are all within the tolerance range, but those of the parts treated by the other two routes are not within the tolerance range.

From the aforementioned comparisons, it can be concluded that the dimensional accuracies of the undried parts treated by route II are the highest for the peripheral dimensions and the diameter of the central hole. Nevertheless, its corresponding dried part can also basically meet the accuracy requirements. But in the usage of the plate, moisture should be prohibited to ensure its insulating and antibreakdown properties; hence, re-drying after the boiling water bath is recommended.

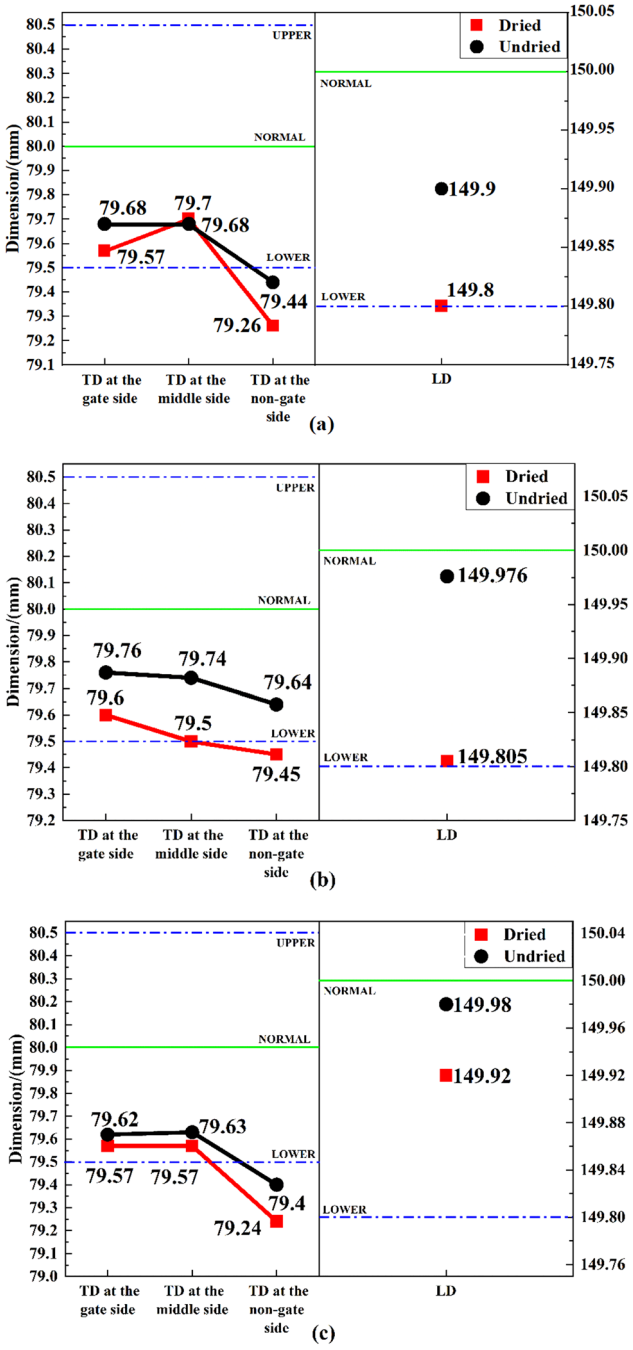

Figure 7: The transverse and longitudinal peripheral dimensions of the plate treated by the three routes: (a) I, (b) II, and (c) III.

4.2 Mechanical property improvements of the plate treated by the three routes

Figure 8 shows the tensile, bending, and impact properties of the plate treated by the three routes. It can be seen that the mechanical properties of the plate have been significantly improved after the boiling water bath. It is because that hygrothermal conditioning treatments reduce the residual stress [15,19,25], which is mainly caused by the "supporting mold." In addition, re-drying can also significantly improve the mechanical properties of the plate [15,25]. However, it should be considered that the impact strength of the dried parts treated by route III, in which the "supporting mold" is added after boiling

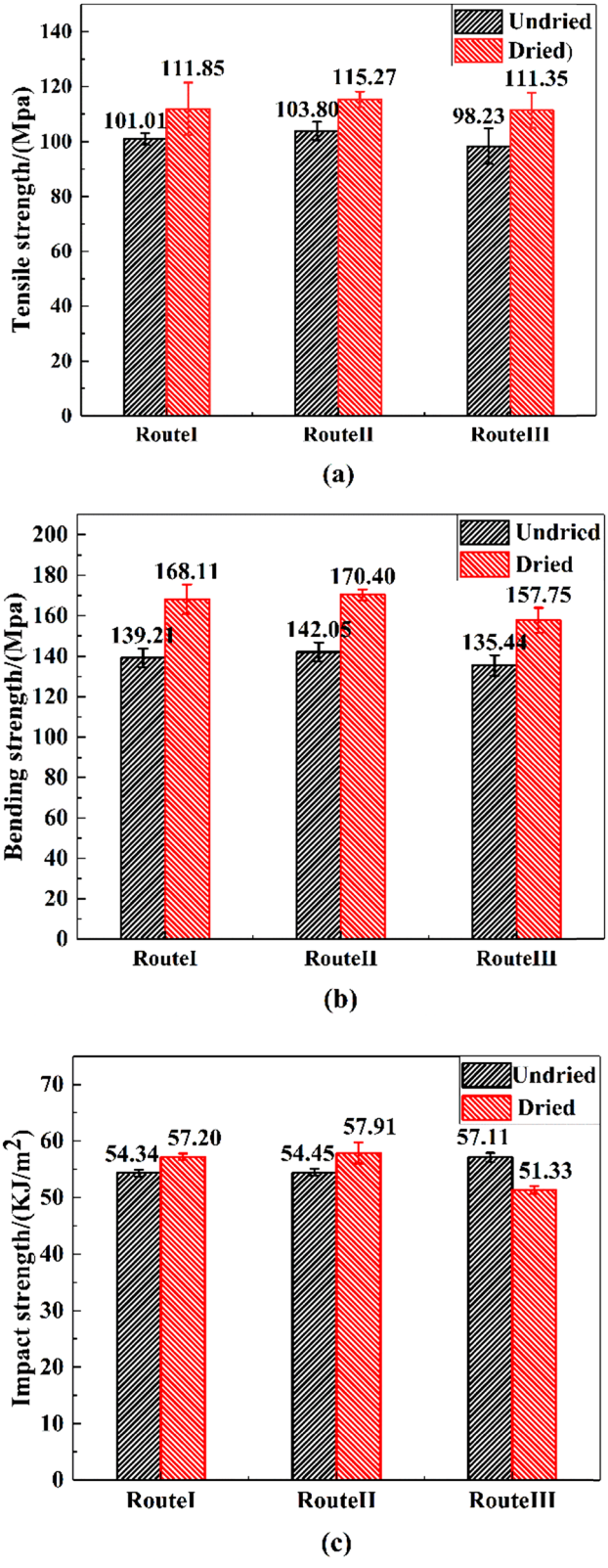

Figure 8: (a) Tensile strength, (b) bending strength, and (c) impact strength of the plate treated by the three routes.

water bath, is lower than that of its corresponding undried parts. It indicates that boiling water bath plays a key role in improving the impact strength. As a result, in route III, the active effect of re-drying on the impact strength, right after the "supporting mold," cannot eliminate the negative effect of the "supporting mold" without a subsequent boiling water bath. Compared with the values before the treatments, Figure 8 and Table 3 show that the tensile strength and bending strength of the dried parts treated by route II increased by more than 141.15 and 159.79%, respectively, even though the impact strength was reduced by 6.37%, which still can meet the requirements for use. Thus, it can be concluded that among the three treatment routes, route II can improve the mechanical properties the best. Boiling in a water bath allows the macromolecule inside the composite to return to its natural orientation as far as possible, and the internal crystallization and decrystallization reach a balance, eliminating the residual stress of the material [15,18,24].

4.3 XRD results obtained for the dried plate treated by the three routes

To further study the effect of the three treatment routes on the crystallization behavior of the dried plate to ensure the employment character, an XRD analysis was carried out subsequently. Figure 9 shows the shape of the XRD peak observed for the composite. It can be seen that three diffraction peaks are observed from the PA66 composite pattern and the shapes are the same basically, which indicates that the treatment routes do not change the phase structure of the PA66 composite. Two characteristic diffraction peaks at 2θ values of 20.3° and 23.5° can be observed, corresponding to α_1 and α_2 crystal phases of PA66 composite, respectively [24]. In addition, there is a diffraction peak corresponding to the γ phase at 2θ values of 28.5°. It indicates that the crystal of the PA66-GF25 FR (RP) composite is a mixture of α and γ phases. At the same time, compared with the untreated composite, the diffraction peaks of the treated ones by the three routes all shifted to varying degrees, and the peak strength increased significantly and the shape became wider, which indicates that the treatment routes could improve the crystallization property of the PA66-GF25 FR (RP) composite [12,25–27].

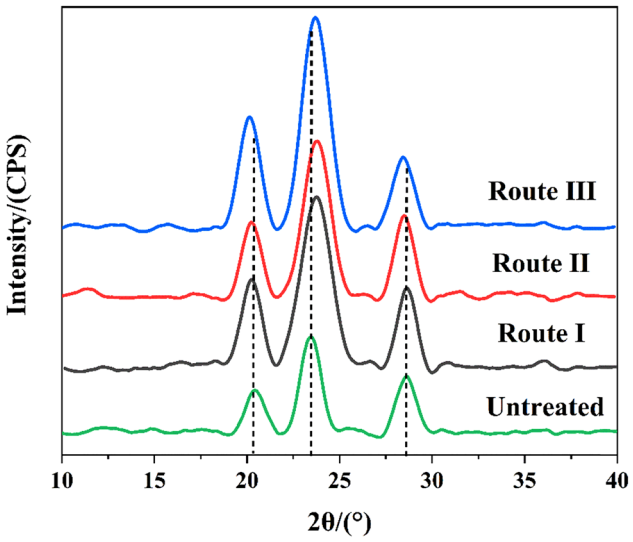

Figure 9: The XRD patterns of the plate.

4.4 Microstructure analysis and of the dried plate treated by the three routes

To further evaluate the effect of the three treatment routes on the mechanical properties of the dried plate, the tensile fracture surface morphologies of the samples were analyzed by SEM, as shown in Figure 10. First, it can be found from the high magnification SEM images (Figure 10(d)–(f)) that a certain amount of PA66 adheres to the fibers, which indicates that the interface bonding of the composite is not reduced by water absorption [19–22].

Figure 10(a) shows that the dimples of the PA66 matrix treated by route I are shallow and disordered. Some thick holes clutter in some regions, and even some deep cracks can be observed, with some of the fibers outside of the matrix indicating that some of the fibers are pulled out and can no longer bear any more

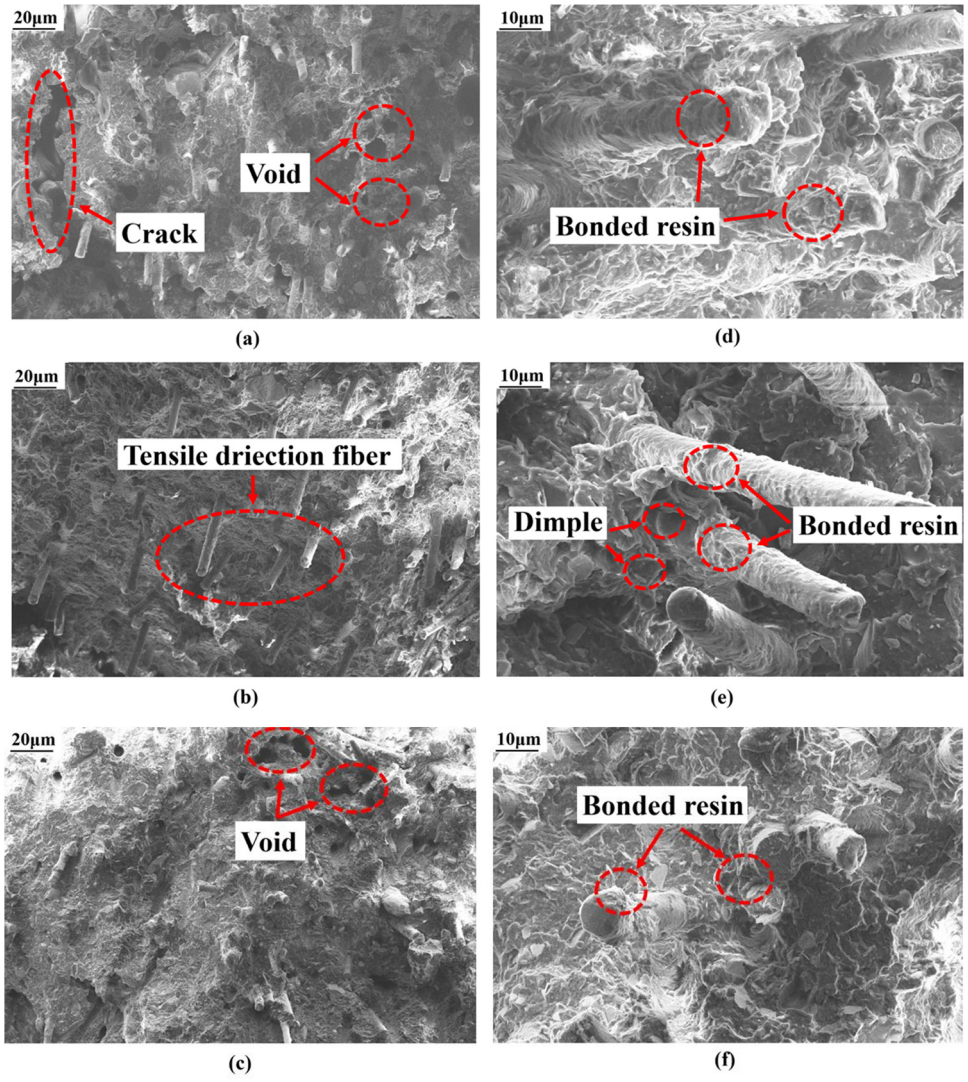

Figure 10: Surface fractography of the plate treated by the three routes: (a) and (d) route I (b), (e) route II, and (c) and (f) route III, in which (a)–(c) were obtained with a magnification of 500, and (d)–(f) were obtained with a magnification of 1,000 times.

Table 4: Final functional performance of the plate

Number	Property	Demand	Test result
1	Functional performance at high and low temperature	10 cycles, in every cycle: −40 to 130°C, 10°C/h, the highest and lowest temperatures were maintained for 4 h, room temperature was maintained for 2 h.	Without cracking or peeling After high and low temperature
2	Power-frequency voltage-withstand test	42 kV	Up to 58 kV
3	Lightning impulse	Phase, opposite: 75 kV Fracture: 85 kV	Phase, opposite: 95 kV Fracture: 110 kV
4	Partial discharge test	Singleton: ≤3PC Whole machine: ≤16PC	Singleton: 0.8–1.8PC Whole machine: 4.2–5.1PC
5	Leak test	$\leq 1.2 \times 10^{-8}$	5.8×10^{-11}
6	Mechanical life test	≥10,000	Qualified
7	Flame-retardant properties	GB/T 2408-1996, ≥V-1	V-0

force during the stretching. Therefore, the adjacent matrix has to bear the load again, and brittle cracks occur prematurely. As a result, the tensile strength of the dried plate treated by route I is the lowest compared to the other treatment routes. Figure 10(b) clearly shows that the dimples of the PA66 matrix are deep and uniform, and the PA66 matrix contains few holes. It can also be seen that the fibers were elongated along the tensile direction, bearing most of the tensile force until the fibers break. Furthermore, it can be seen that there is less resin on the fibers on the fracture surface treated by route II, whose tensile strength is the highest (Figure 8(a)). Route II achieves the highest tensile strength among the three routes because the PA66 matrix treated by route II is stronger than the PA66 matrix treated by the other routes, and the failure mode changes from matrix fracture to interfacial fracture before the elongated fibers break [24]. Figure 10(c) shows that the matrix of the tensile fracture surface treated by route III is flat; the dimples are very shallow, indicating a brittle fracture of the matrix. Moreover, the fibers shown in Figure 10(c) do not elongate as much as those in Figure 10(a) and (b). Both the GFs and the PA66 matrix treated by route III experience brittle fracture, verifying the lower strengths and low impact strength of the dried parts.

4.5 Functional performance

To verify the functional performance of the plate in the medium voltage switch. According to GB/T 11022-2011 (Common Specifications for High-Voltage Switchgear and Controllable Standards), the necessary performance tests were carried out for the re-dried plate treated by route II, as presented in Table 4.

From the comparison and analysis of the three routes, it can be concluded that the re-dried plate treated by route II is preferred for ensuring the dimensional accuracies, mechanical properties, and the employment character of the medium voltage environment.

5 Conclusion

In this article, three different treatment routes were applied and analyzed after injection molding to study the roles of boiling water bath and re-drying in improving the dimensional accuracies and mechanical properties of a plate that was made of PA66-GF25 FR (RP) by performing size measurements, mechanical property tests, and micro-morphology comparisons. Some conclusions are presented here.

The addition of a “supporting mold” can inhibit the continuous linear shrinkage of the composite to a certain extent, improving the dimensional accuracies of the product; however, at the same time, it will increase the residual internal stress inside the products and lead to a serious decline in the mechanical properties. Boiling water bath at 90–100°C can balance the crystallization and decrystallization of polyamide, thereby simultaneously reducing the residual internal stress and the linear shrinkage, improving the mechanical properties and dimensional accuracies.

By comparing the effects of the three different treatment routes on the dimensional accuracy, mechanical properties, and microstructures of PA66-26GF FR (RP) composites, it can be found that treatment route II, in which a “supporting mold” is added and boiling water bath is subsequently performed, can result in the highest

dimensional accuracy, the best mechanical properties, and the best micro-morphology, which include the least pulled-out and the maximum elongation of fibers, the deepest dimples, indicating the best strength of the matrix and the best interfacial bonding of the matrix and the fibers.

Re-drying at 110°C for 6 h can further enhance the mechanical properties of the PA66-26GF FR (RP) composite as a whole mainly because of the reduction in the internal residual stress. The functional performances can be ensured after the plate is treated by the "supporting mold," boiling water bath, and re-drying.

Acknowledgments: This work was financially supported by the National Natural Science Foundation of China (51705295 and 51778351), The Shandong Provincial Natural Science Foundation, China (ZR2020KE013 and ZR2018MEE022), and University QingChuang science and technology plan of Shandong (2019KJB015).

Conflict of interest: The authors state no conflict of interest.

Data availability statement: The datasets generated during and/or analyzed during the current study are available from the corresponding author on reasonable request.

References

[1] Rudresh BM, Ravikumar BN. Effect of short glass fibers loading on the mechanical behaviour of PA66/PTFE blend composites. Trans Indian Inst Met. 2017;70(5):1285–94.
[2] Yang B, Leng JH, He BB, Liu H, Zhang Y, Duan ZH. Influence of fibers length and compatibilizer on mechanical properties of long glass fibers reinforced polyamide 66. J Reinforced Plast Compos. 2012;31(16):1103–12.
[3] Thomason JL. Structure–property relationships in glass reinforced polyamide, part 2: The effects of average fibers diameter and diameter distribution. Polym Compos. 2007;28(3):331–43.
[4] Zhang SH, Cui C, Chen G. Tribological behavior of MC nylon6 composites filled with glass fiber and flyash. J Wuhan Univ Technology-Materials Sci Ed. 2012;2:290–5.
[5] Jou WS, Chen KN, Chao DY, Lin CY, Yeh JT. Flame retardant and dielectric properties of glass fibre reinforced nylon-66 filled with red phosphorous. Polym Degrad Stab. 2001;74(2):239–45.
[6] Liu Y, Qi Wang. Melamine cyanurate-microencapsulated red phosphorus flame retardant unreinforced and glass fibers reinforced polyamide 66. Polym Degrad Stab. 2006;91(12):3103–9.
[7] Fan HL, Guan DH, Cao YQ, Wang ZY. Effect of flame retardant on properties of glass fibers reinforced polyamide 66. Eng Plast Application. 2002;10:9–11.
[8] Adriano Damiani R, Fiori J, Silvano JR, Neto ABSS, de Araújo PHH, Riella HG, et al. Influence of the injection molding process on the mechanical properties of (PA6/GF/MMT) nanocomposite. Polym Compos. 2015;36(2):237–44.
[9] Lafranche E, Krawczak P, Ciolczyk JP, Maugey J. Injection moulding of long glass fibers reinforced polyamide 66: processing conditions/microstructure/flexural properties relationship. Adv Polym Technol. 2005;24(2):114–31.
[10] Teixeira D, Giovanela M, Gonella LB, Crespo JS. Influence of flow restriction on the microstructure and mechanical properties of long glass fibers-reinforced polyamide 6.6 composites for automotive applications. Mater Des. 2013;47:287–94.
[11] Coulon A, Lafranche E, Douchain C, Krawczak P, Ciolczyk J, Gamache E. Flexural creep behaviour of long glass fibre reinforced polyamide 6.6 under thermal-oxidative environment. J Composite Mater. 2017;51(17):2477–90.
[12] Clavería I, Elduque D, Santolaria J, Pina C, Javierre C, Fernandez A. The influence of environmental conditions on the dimensional stability of components injected with PA6 and PA66. Polym Test. 2016;50:15–25.
[13] Thomason JL, Ali JZ, Anderson J. The thermo-mechanical performance of glass-fibre reinforced polyamide 66 during glycol-water hydrolysis conditioning. Compos Part A. 2010;41(7):820–6.
[14] Humeau C, Davies P, Legac PY, Jacquemin F. Influence of water on the short and long term mechanical behaviour of polyamide 6(polyamide) fibres and yarns. Multiscale Multidiscip Modeling, Exp Des. 2018;1(4):317–27.
[15] Bian XS, Ambrosio L, Kenny JM, Nicolais L, Dibenedetto AT. Effect of water absorption on the behavior of E-glass fibers/nylon-6 composites. Polym Compos. 1991;12(5):333–7.
[16] Rajeesh KR, Gnanamoorthy R, Velmurugan R. The effect of moisture content on the tensile behaviour of polyamide6 nanocomposites. Mater Des Appl. 2010;224(12):173–6.
[17] Thomason JL. Structure-property relationships in glass-reinforced polyamide, part 3: effects of hydrolysis ageing on the dimensional stability and performance of short glass-fibers-reinforced polyamide 66. Polym Compos. 2007;28(3):344–54.
[18] Autay R, Njeh A, Dammak F. Effect of hygrothermal aging on mechanical and tribological behaviors of short glass-fibers-reinforced PA66. J Thermoplast Compos Mater. 2019;32(12):1585–1600.
[19] Eftekhari M, Fatemi A. Tensile behavior of thermoplastic composites including temperature, moisture, and hygrothermal effects. Polym Test. 2016;51:151–64.
[20] Yang SL, Liu WQ, Fang Y, Huo RL. Influence of hygrothermal aging on the durability and interfacial performance of pultruded glass fibers-reinforced polymer composites. J Mater Sci. 2019;54(3):2102–21.
[21] Bergeret A, Ferry L, Ienny P. Influence of the fibre/matrix interface on ageing mechanisms of glass fibre reinforced

thermoplastic composites (PA-6,6, PET, PBT) in a hygro-thermal environment. Polym Degrad Stab. 2009;94(9):1315–24.
[22] Bergeret A, Pires I, Foulc MP, Abadie B, Ferry L, Crespy A. The hygrothermal behaviour of glass-fibre-reinforced thermoplastic composites: a prediction of the composite lifetime. Polym Test. 2001;20(7):753–63.
[23] Keating MY, Malone LB, Saunders WD. Annealing effect on semi-crystalline materials in creep behavior. J Therm Anal Calorim. 2002;69(1):37–52.
[24] Meng QY, Gu YZ, Luo L, Wang SK, Li M, Zhang ZG. Annealing effect on crystalline structure and mechanical properties in long glass fibers reinforced polyamide 66. J Appl Polym Sci. 2017;134(13):1–10.
[25] Seltzer R, Frontini PM, Mai YW. Effect of hygrothermal ageing on morphology and indentation modulus of injection moulded nylon 6/organoclay nanocomposites. Compos Sci Technol. 2009;69(7–8):1093–1100.
[26] Lu YL, Zhang Y, Zhang GB, Yang MS, Yan SK, Shen DY. Influence of thermal processing on the perfection of crystals in polyamide 66 and polyamide 66/clay nanocomposites. Polymer. 2004;45(26):8999–9009.
[27] Wolanov Y, Feldman AY, Harel H, Marom G. Amorphous and crystalline phase interaction during the Brill transition in nylon 66. Express Polym Lett. 2009;3(7):452–7.
[28] Feldman AY, Wachtel E, Vaughan GBM, Weinberg A, Marom G. The Brill transition in transcrystalline nylon-66. Macromolecules. 2006;39(13):4455–9.